

Determination of step-edge orientation by helium atom scattering

M. Patting, D. Fariás,* and K. H. Rieder

Fachbereich Physik, Freie Universität Berlin, Arnimallee 14, D-14195 Berlin, Germany

(Received 9 March 2000)

Helium atom scattering (HAS) has been used to determine the step-edge orientation on a Rh(311) surface, whose close-packed rows are separated by alternating (100) and (111) microfacets. The measurements were performed on a surface in which the step density was previously increased by sputtering. Intense additional peaks were observed at $\sim 48^\circ$ and $\sim 56^\circ$ from the specular beam when the incident He beam was impinging on the (100) or (111) microfacets, respectively. The same behavior was observed at different He energies and angles of incidence, demonstrating that the observed peaks are caused by specular diffraction at uphill step edges. The step height could also be determined from the appearance of additional maxima at higher He energies. These results allow us to determine the in-plane scattering geometry in HAS studies of stepped surfaces in a very simple way.

I. INTRODUCTION

Helium atom scattering (HAS) has been developed in the last decade into a powerful tool for investigating the structure¹ and dynamics² of clean and adsorbate covered surfaces. Because of the low energies used (10–300 meV), the incident He atoms probe the topmost layer of the substrate surface in an absolutely nondestructive manner, and are equally applicable to insulators, semiconductors, and metals. Results obtained in recent years demonstrate that HAS is also a unique technique for the study of structural disorder on surfaces.³ In effect, the attenuation of the specular intensity by single adatoms on a smooth surface is characterized by a giant cross section of $\sim 100 \text{ \AA}^2$, whereas step edges are “seen” by He atoms as 10-\AA -wide strips. This attenuation is almost entirely due to small-angle scattering around the specular direction (caused by long-range interactions in the He-surface system), and allows one to gain a wealth of information on growth and diffusion studies.^{1,3} A different approach in investigating defects on surfaces consists of looking at the small fraction of intensity scattered through larger angles, which results from short-range repulsive forces and yields geometrical information on the surface defect.^{4–8} These large-angle oscillations in the angular intensity distribution are more difficult to observe experimentally because of their low intensities (typically 10^{-3} – 10^{-4} of the specular intensity), and were first observed by Lahee *et al.* from a randomly stepped Pt(111) surface⁷. Due to their low intensity, these features were previously investigated only on smooth surfaces like the fcc(111) and fcc(100), whose diffraction patterns consist merely of the specular beam.

In our current work we have applied HAS to characterize step edges on a sputtered Rh(311) surface. This is an open, highly corrugated surface, which consists of close-packed rows separated by alternating (111) and (100) microfacets (Fig. 1). In view of the bulk values, the (100) facets are tilted by 25.24° with respect to the surface plane, whereas the (111) facets are tilted by 29.50° . The observation of specular diffraction from these two facets allows one to determine whether the incident He beam impinges against the (111) or (100) facets, a distinction which cannot be made by analyz-

ing diffraction from the terraces, since a symmetric corrugation function is obtained for both scattering geometries.^{9,10} Also, the step height can be determined from the appearance of additional maxima in the spectra at higher incident energies. These results are also supported by eikonal calculations.

II. EXPERIMENT

The He-scattering apparatus used in our investigations was described in detail in Ref. 11. The measurements were carried out with pressures of 80 bar behind the nozzle, and nozzle temperatures between 300 and 800 K corresponding to wavelengths of 0.55 – 0.34 \AA . The base pressure in the scattering chamber was 7×10^{-11} mbar, rising to 2×10^{-10} mbar with the He beam on. The scattered He atoms were detected using a quadrupole mass spectrometer which is

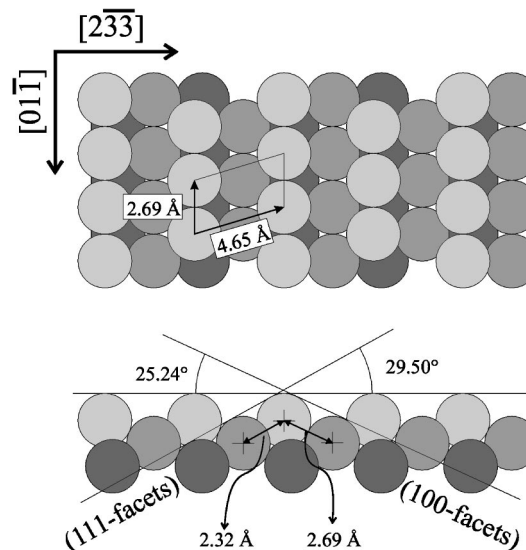


FIG. 1. Sphere model of the Rh(311) surface. A fcc(311) surface consists of alternating (111) and (100) microfacets which are tilted by slightly different angles with respect to the surface normal (bottom).

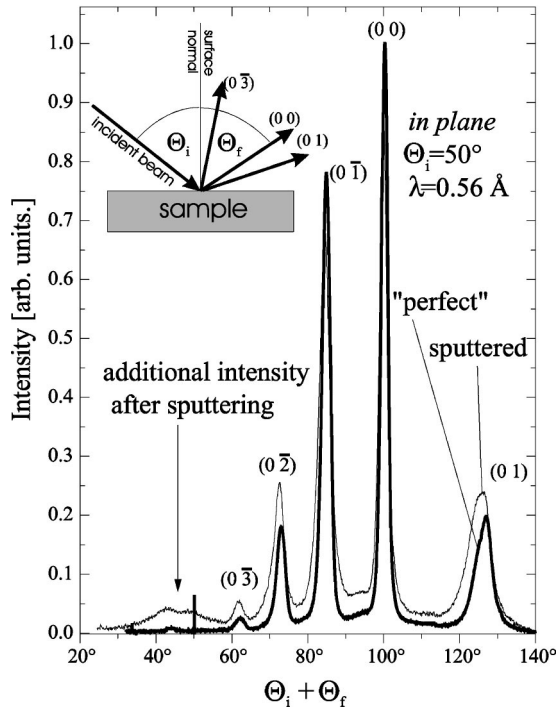


FIG. 2. Comparison between the in-plane spectra of a “perfect” Rb(311) surface and a sputtered Rh(311) surface. Note the additional intensity at $\sim 45^\circ$ observed for the sputtered surface, which appears very close to normal emergence (indicated by a vertical line at 50°). The incoherent background increases, and the peaks become broader after sputtering; however, the relative diffraction intensities remain essentially unchanged.

mounted on a two-axis goniometer. The spectra were taken at a fixed scattering geometry, with the incoming beam impinging perpendicular to the close-packed rows of the Rh(311) surface. All spectra shown here have been recorded in the incidence plane, i.e., in the plane defined by the incident beam and the normal to the surface. Incidence and scattering angles are measured with respect to the surface normal (see the inset of Fig. 2).

The Rh(311) surface was aligned to $\pm 0.3^\circ$ with x rays, cut with a wire saw, and mechanically polished. It was initially prepared by repeated cycles of Ne-ion sputtering and annealing to 1100 K. Daily preparation consisted of 30-min sputtering, followed by heating 5 min in 1×10^{-8} -mbar oxygen at 1000 K and 10 min in 1×10^{-8} mbar hydrogen at 500 K. Sample cleanliness was indicated by optimum He reflectivity and the shape of the spectra, narrow beams and weak incoherent background indicating a well-prepared surface. The density of steps at the surface was increased by sputtering at 100 K for 5 min, and subsequent flash annealing to 430 K. Complete removal of the steps was achieved by heating to 1000 K for 15 min.

III. RESULTS AND DISCUSSION

Figure 2 shows a comparison between the spectra recorded with a room-temperature He beam from a “perfect” Rh(311) surface and a sputtered surface. The scattering geometry was such that the incoming He beam impinged against the (100) facets, according to a previous structure determination with x-ray scattering. The total in-plane elastic

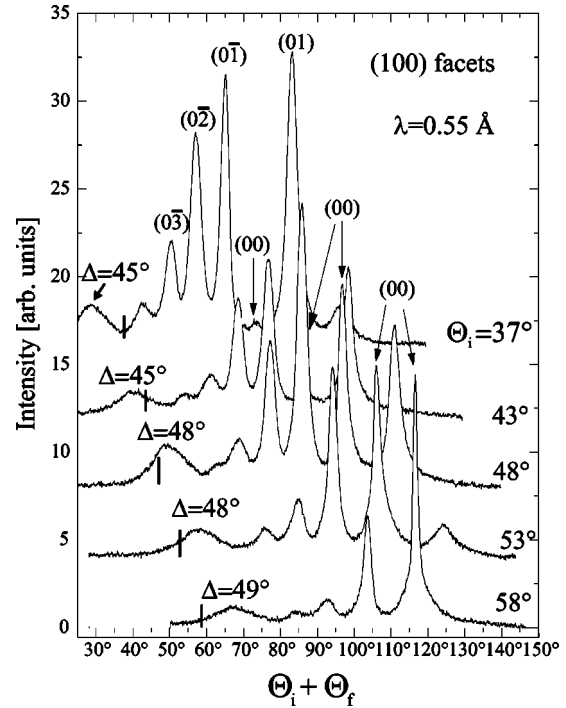


FIG. 3. Spectra recorded for the sputtered surface with the He beam impinging on the (100) facets at several incident angles. Δ denotes the distance between the additional maximum and the specular beam. A value of $\Delta \sim 47^\circ$ is observed for all angles of incidence, suggesting that this peak arises from specular diffraction at (100) step edges. The vertical lines on the left part of all spectra indicate the normal emergence condition $\Theta_f = 0^\circ$.

intensity has been normalized to unity in the two spectra to allow a better comparison. As expected, the sputtered surface gives rise to a significantly stronger incoherent background; the diffraction beams become broader, whereas their relative intensities remain essentially unchanged compared to the “perfect” surface. The beam broadening indicates that the ordered domains become smaller after sputtering, whereas the increased background is caused by an increased density of defects. The most impressive change induced by sputtering is the appearance of an additional scattered intensity marked by an arrow in the spectrum shown in Fig. 2, very close to normal emergence (corresponding to $\Theta_f = 0^\circ$). The peak’s height was found to depend mainly on how long the surface was sputtered, and at which temperatures it was annealed afterwards. The position of the additional peak, however, remained unchanged, independently of the details of preparation. The splitting of the peak is discussed later.

To elucidate the origin of these peaks we measured spectra at different angles of incidence. In contrast with the behavior expected for a diffraction beam, this feature retained a constant angular separation from the specular beam; for the experimental conditions of Fig. 3 this distance is $\sim 47^\circ$. The vertical lines on the left part of all spectra indicate the condition $\Theta_f = 0^\circ$, to stress the fact that the additional intensity appears very close to normal emergence. Due to its broad form, the position of this peak’s maximum could not be determined with great accuracy. Since the intensity of the additional peaks decreases rapidly with increasing azimuthal angle (the angle measured away from the plane of incidence), we conclude that the sputtering/annealing process

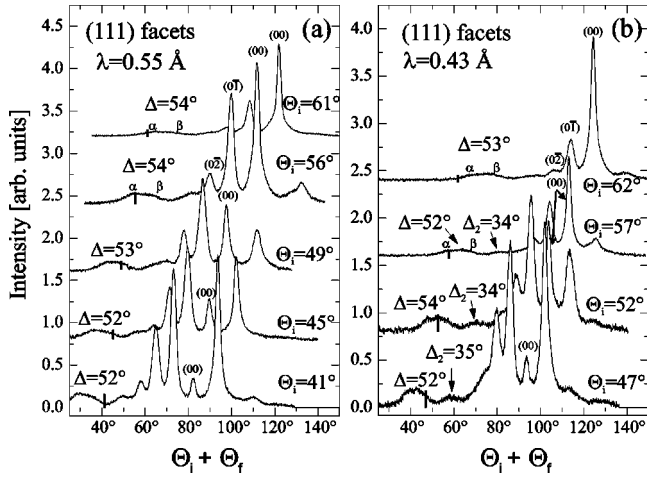


FIG. 4. (a) Same as Fig. 3 after rotating the sample by 180° around the surface normal. The additional intensity now appears at $\Delta \sim 53^\circ$, which is consistent with specular diffraction from (111) facets. (b) Same as (a), but with an incident wavelength of 0.43 \AA . Unlike a diffraction beam from the Rh(311) surface, the additional peak still appears at $\Delta = 53^\circ$. Moreover, a second additional maximum Δ_2 is revealed at this energy, as well as a splitting of the additional peak denoted by α and β . The vertical lines on the left part of all spectra indicate the normal emergence condition $\Theta_f = 0^\circ$.

has produced steps parallel to the close-packed rows. The observed additional peaks could then be explained as arising from specular scattering at uphill step edges. The angle of inclination of these step edges with respect to the terrace direction, $\alpha_{[100]}$, can then be determined from the position of the additional peak's maximum with respect to the specular beam, Δ . From simple geometrical considerations one obtains $\alpha_{[100]} = \Delta/2 = (24 \pm 1)^\circ$. This value is consistent with the orientation expected for (100)-facet step edges (Fig. 1).

This behavior resembles in many aspects the reflection-symmetry interferences observed on lower corrugated surfaces, with intensities of the order of 10^{-3} – 10^{-4} of the specular intensity.^{4–8} However, the large amount of intensity observed points to a rather different physical origin in our case. A triangular background can be observed near the specular beam in some spectra, which may be attributed to a random distribution of defect sites after sputtering, as already reported for Ni(100)- $c(2 \times 2)$ O by Schlup and Rieder.¹² In what follows we will describe a series of results which give further support to our interpretation of the additional feature in Figs. 2 and 3 in terms of specular scattering at step edges. According to this, it should also be possible to detect specular scattering from (111) facets. Note that, for typical scattering conditions ($\theta_i > \alpha$), only specular scattering from uphill steps in the backward scattering direction (i.e., in the direction of negative parallel momentum transfer) is to be expected. Thus, to detect scattering at the (111) facets, the sample must be rotated 180° around its normal, so that the incoming beam could directly impinge on the (111) facets.

Figure 4(a) shows the result of such measurements. The additional peaks are again visible, but the distance to the specular beam has now increased to $\Delta \sim 53^\circ$. This leads to an orientation angle $\alpha_{[111]} = (27 \pm 1)^\circ$, which indeed is consistent with the expected value for (111) facets. Unlike the scat-

tering at the (100) facets a more or less distinct splitting of the additional peak is seen; the two features are denoted as α and β in Fig. 4. Note that almost identical diffraction spectra are recorded for both possible sample orientations, so that they do not offer any possibility to decide whether the incoming beam impinges on the (111) or (100) facets. Actually, it is a well-known fact that symmetric corrugation functions are obtained with He diffraction even for very asymmetric stepped surfaces [as for example, Cu(117)], so it is not possible to decide on which microfacet the incoming beam is impinging by analyzing the angular intensity distributions.¹ The method proposed here would allow one to overcome this problem *in situ* for high Miller-index surfaces, avoiding the need of a previous orientation using x-ray scattering.

Further support for our interpretation is given by the spectra shown in Fig. 4(b), which were recorded with a higher incident beam energy corresponding to a wavelength $\lambda = 0.43 \text{ \AA}$. The additional maximum appears at the same position ($\Delta \sim 53^\circ$), indicating that it cannot be a high-order diffraction beam, because in this case the maximum should have decidedly moved toward the specular beam. Another interesting feature not visible at $\lambda = 0.55 \text{ \AA}$ can be seen in these spectra: a well-resolved second ‘‘additional’’ maximum, visible, for example, in the lowest spectrum ($\Theta_i = 47^\circ$) at $\Theta_f = 60^\circ$. This feature can be resolved using a shorter wavelength due to the shift of the Rh(311) diffraction beams toward the specular beam. Similarly to the main additional maximum at $\Delta \sim 53^\circ$, the second one keeps a fixed distance of $\Delta_2 \sim 34^\circ$ independently of the angle of incidence. If the step edge is considered to be a single slit, the second maximum can then be attributed to first-order diffraction by the slit, and as a consequence may allow a determination of the slit width.

To confirm this assumption, we measured spectra at several different wavelengths and angles of incidence with the incoming beam impinging on the (111) facets [Figs. 5(a) and 5(b)]. The main additional maximum stays at the same angle as λ varies, supporting our interpretation of this feature as specular scattering from (111) facets. The second additional maximum, in contrast, moves away from the main maximum with increasing wavelength, as shown by the dotted lines at $\sim 45^\circ$ in Fig. 5(a) and $\sim 92^\circ$ in Fig. 5(b). If it were a high-order diffraction beam of the Rh(311) surface, it should move away from the specular beam, i.e., in the opposite direction. On the other hand, a beam diffracted by a single slit should move in the observed direction. In the topmost spectrum of Fig. 5(b), corresponding to $\lambda = 0.56 \text{ \AA}$, the second additional maximum overlaps with the $(0\bar{2})$ beam of the Rh(311) surface, making its detection possible only at shorter wavelengths. In order to obtain the slit width from these data, all we need are equations describing the diffraction of a beam of wavelength λ incident on a slit of width d with an angle Θ_i^* .¹³ The diffraction maxima of order n appear at angles Θ_f^* , satisfying

$$\sin \Theta_{fn}^* = \frac{\pm \left(\frac{1}{2} + n \right) \lambda}{d} + \sin \Theta_i^*, \quad n = 1, 2, 3, \dots \quad (1)$$

For the angles of destructive interference it holds that:

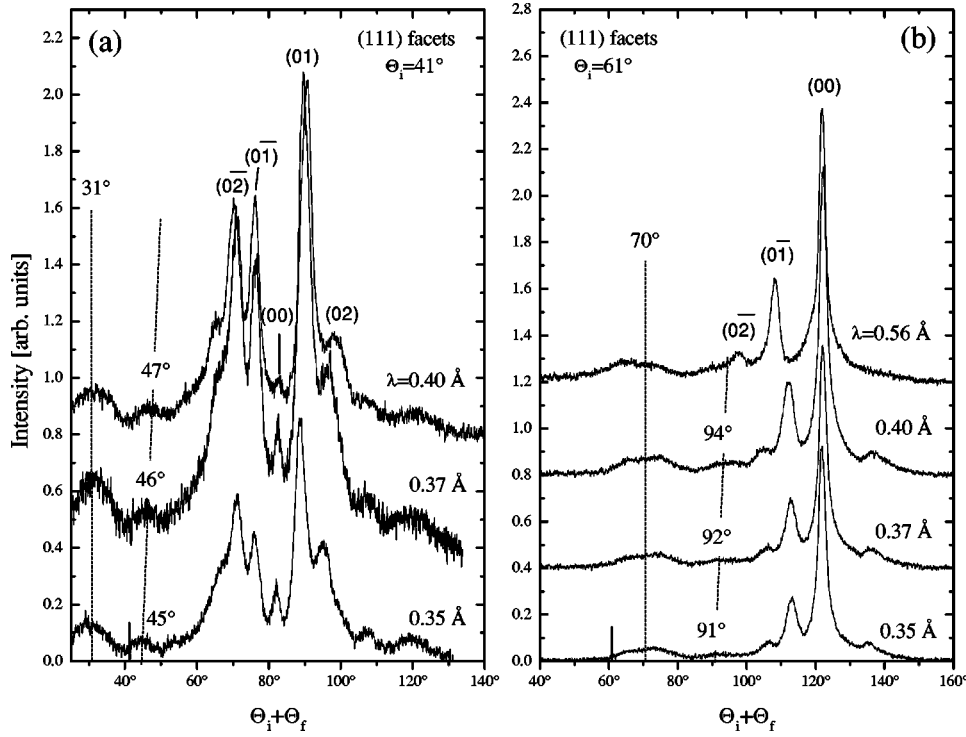


FIG. 5. Spectra recorded at two different incident angles and several different wavelengths. The main maximum remains at the same position - 31° and 70° in (a) and (b), respectively, whereas the second maximum drifts away from the first one with increasing wavelength, as indicated by the dotted lines at $\sim 45^\circ$ in (a) and $\sim 92^\circ$ in (b). We conclude that the latter maximum is to be interpreted as the first-order intensity scattered off a step acting as a single slit. The vertical lines on the left part of the lowest spectra indicate the normal emergence condition $\Theta_f = 0^\circ$.

$$\sin \Theta_{An}^* = \frac{n\lambda}{d} + \sin \Theta_i^*, \quad n = \pm 1, 2, 3, \dots \quad (2)$$

Table I summarizes the positions of the maxima in Figs. 5(a) and 5(b) with respect to the normal of the (111) facet. From Eqs. (1) and (2) we calculated the corresponding step width. We found $d = 2.17 \pm 0.5 \text{ \AA}$, corresponding to a step height of $h = 0.9 \pm 0.1 \text{ \AA}$, which is in good agreement with the value $h = 1.1 \text{ \AA}$, which is the height expected for monoatomic steps on a bulk-terminated Rh(311) surface.

We also performed some simple eikonal calculations in which we modeled the Rh(311) surface with a cosine of height 0.3 \AA and the step by a slope embedded in a 24-\AA -wide area (Fig. 6, inset). The maximum corrugation ampli-

tude used in the simulations was taken from a previous HAS study of the clean Rh(311) surface.⁹ In these studies the intensity analyses were performed with the GR method within the hard-corrugated wall model; however, in view of the small corrugation amplitude compared to the surface lattice constant the use of the computationally simpler eikonal approximation in our simulations is also well justified.¹ For a

TABLE I. Positions of the additional maxima for several wavelengths (λ) and incident angles (Θ_i) for the (111) facet. Θ_i^* is the incident angle with respect to the facet normal, Θ_{A1}^* is the first angle of destructive interference, and Θ_{f1}^* is the position of the first maximum. These angles were determined from the position of the main additional peak in the He diffraction data.

Fig.	λ	Θ_i	Θ_i^*	Θ_{A1}^*	Θ_{f1}^*
4(b)	0.43 \AA	47°	20°	32°	39°
	0.43 \AA	52°	26°	38°	45°
	0.43 \AA	57°	30°	45°	51°
	0.43 \AA	62°	36°	51°	60°
5(a)	0.38 \AA	41°	15°	26°	33°
	0.41 \AA	41°	15°	25°	31°
	0.44 \AA	41°	15°	26°	30°
5(b)	0.38 \AA	61°	34°	50°	59°
	0.41 \AA	61°	34°	50°	59°
	0.44 \AA	61°	34°	52°	59°

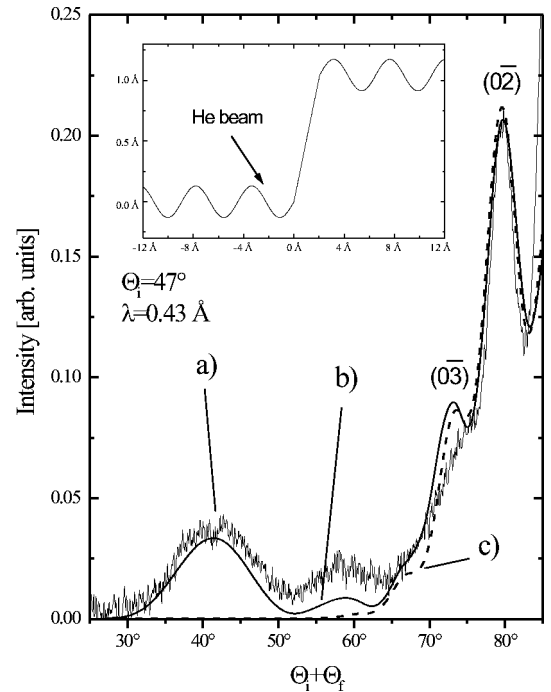


FIG. 6. Results of eikonal simulations (b) for the model surface shown in the inset (note the different vertical and horizontal scales). The position and height of both maxima agree well with experiment (a), whereas they are not observed for a model surface without step (c).

better comparison with experiment the calculated spectra were smoothed to simulate the broadening of the beams caused by resolution limiting factors, like the finite width of the incoming beam and the large aperture placed in front of the mass spectrometer. In Fig. 6 the results of our simulations for a model surface (b) are compared to a He-diffraction pattern (a). Note that the position and height of both maxima agree well with the experimental data, whereas they are not present for calculations on a model surface without step (c). Despite the simplicity of our model, the most salient features in experiment are well reproduced by the calculations, providing support to our interpretation of the additional features observed in the spectra.

The main additional peak's splitting observed for scattering on (111) step edges (Fig. 4, marked as α and β) points to the presence of two slightly different facet orientations on the surface. For α results an orientation of $(28.3 \pm 0.3)^\circ$, whereas a value of $(24.9 \pm 0.3)^\circ$ is obtained for β . The reason for the presence of two different orientations is the following: Monoatomic steps will lead to a less tilted step edge compared with a (111) facet due to a smoothing of the surface charge density at the steps (the Smoluchowski effect) which is more pronounced in the case of He atoms, since they are scattered at a distance of $\sim 4 \text{ \AA}$ from the surface atom cores. These effects are expected to be less important for double steps than for single steps. As a consequence, an orientation of $(24.9 \pm 0.3)^\circ$ is seen for monoatomic steps, whereas a value of $(28.3 \pm 0.3)^\circ$ [closer to an ideal (111) orientation step] is obtained for double steps. Since double

steps have been only observed with the He beam impinging on the (111) facets, our results suggest that the formation of (100) double steps may be thermodynamically unfavorable. Unfortunately, a higher-order additional intensity was not observed for double steps, probably because it is buried at least partly beneath the main additional peak.

IV. CONCLUSIONS

We observed helium atom scattering from step edges on the highly corrugated Rh(311) surface, which led to the appearance of additional peaks in the in-plane diffraction spectra. The main maximum arises from specular diffraction at step-edges, whereas a second, less intensive maximum observed at higher incident energies is caused by first-order diffraction at step edges acting as single slits. From the position of this peak, the step height could also be determined. The most salient features in experiment have been well reproduced by eikonal calculations. In particular, these results allow to determine whether the He beam is impinging against the (111) or (100) facets in a simple way, which is not possible from an analysis of diffraction data.

ACKNOWLEDGMENTS

The authors wish to thank J. R. Manson for stimulating and helpful discussions. This work was supported by the Deutsche Forschungsgemeinschaft, Sonderforschungsbereich 290 (TP A5).

*Present address: Departamento de Física de la Materia Condensada, Universidad Autónoma de Madrid, Cantoblanco, 28049 Madrid, Spain.

¹D. Fariás and K. H. Rieder, Rep. Prog. Phys. **61**, 1575 (1998).

²J. P. Toennies, in *Surface Phonons*, Springer Series in Surface Sciences Vol. 21, edited by W. Kress and F. W. de Wette (Springer, Berlin, 1991), pp. 111–116.

³B. Poelsema and G. Comsa, *Scattering of Thermal Atoms From Disordered Surfaces*, Springer Tracts in Modern Physics 115, (Springer, Berlin, 1989).

⁴B. J. Hinch, Phys. Rev. B **38**, 5260 (1988).

⁵B. J. Hinch, A. Lock, J. P. Toennies, and G. Zhang, J. Vac. Sci. Technol. B **7**, 1260 (1989).

⁶B. J. Hinch and J. P. Toennies, Phys. Rev. B **42**, 1209 (1990).

⁷A. M. Lahee, J. R. Manson, J. P. Toennies, and C. Wöll, Phys. Rev. Lett. **57**, 471 (1986).

⁸A. M. Lahee, J. R. Manson, J. P. Toennies, and C. Wöll, J. Chem. Phys. **86**, 7194 (1987).

⁹R. Apel, D. Fariás, and K. H. Rieder, Surf. Rev. Lett. **2**, 153 (1995).

¹⁰D. Fariás, S. Siebentritt, R. Apel, R. Pues, and K. H. Rieder, J. Chem. Phys. **106**, 8254 (1997).

¹¹T. Engel and K. H. Rieder, Surf. Sci. **109**, 140 (1981).

¹²W. A. Schlup and K. H. Rieder, Phys. Rev. Lett. **56**, 73 (1986).

¹³J. M. Cowley, *Diffraction Physics* (North-Holland, Amsterdam, 1984).